International Journal of Nanomedicine

Dovepress
open access to scientific and medical research

Open Access Full Text Article

ORIGINAL RESEARCH

Dual-Channel Detection of Breast Cancer Biomarkers CA15-3 and CEA in Human Serum Using Dialysis-Silicon Nanowire Field Effect Transistor

Hang Li[1,*], Shuai Wang[2,*], Xiaosong Li[1], Cong Cheng[3], Xiping Shen[1], Tong Wang[3]

[1]Department of General Surgery, Suzhou Ninth Hospital Affiliated to Soochow University, Suzhou, Jiangsu Province, People's Republic of China; [2]Department of General Surgery, Affiliated Hospital of Jiangnan University, Wuxi, Jiangsu Province, People's Republic of China; [3]Department of General Surgery, Nanjing Medical University Affiliated Wuxi People's Hospital, Wuxi, Jiangsu Province, People's Republic of China

*These authors contributed equally to this work

Correspondence: Xiping Shen, Department of General Surgery, Suzhou Ninth Hospital Affiliated to Soochow University, Suzhou, Jiangsu Province, 215000, People's Republic of China, Tel +86-512-82881248, Email shenxiping2022@163.com; Tong Wang, Department of General Surgery, Nanjing Medical University Affiliated Wuxi People's Hospital, Wuxi, Jiangsu Province, 214000, People's Republic of China, Tel +86-510-82700778, Email aanti@163.com

Background: Breast cancer (BC) is the most common malignant tumors and the leading cause of cancer deaths among women. The early diagnosis and treatment of BC are effective measures that can increase survival rates and reduce mortality. Carbohydrate antigens 15–3 (CA15-3) and carcinoma embryonic antigens (CEA) have been regarded as the most two valuable tumor markers of BC. The combined detection of CA15-3 and CEA could improve the sensitivity and accuracy of early diagnosis for BC.

Methods: The multi-channel double-gate silicon nanowire field effect transistor (SiNW-FET) biosensors were fabricated by using the top-down semiconductor manufacturing technology. By surface modification of the different SiNW surfaces with monoclonal CA15-3 and CEA antibodies separately, the prepared SiNW-FET was processed into biosensor for dual-channel detection of CA15-3 and CEA.

Results: The prepared SiNW-FET biosensors were proved to have high sensitivity and specificity for the dual-channel detection of CA15-3 and CEA, and the detection limit is as low as 0.1U/mL CA15-3 and 0.01 ng/mL CEA. Moreover, the SiNW-FET biosensors were able to detect CA15-3 and CEA in serum by connecting a miniature hemodialyzer.

Conclusion: The present study reported a SiNW-FET biosensor for dual-channel detection of breast cancer biomarkers CA15-3 and CEA in serum, which has potential clinical application value for the early diagnosis and curative effect observation of BC.

Keywords: breast cancer, dual-channel detection, dialysis, silicon nanowire field effect transistor, carbohydrate antigens 15-3, carcinoma embryonic antigens

Introduction

Breast cancer (BC) is the most common malignant tumors and the leading cause of cancer deaths among women.[1] Moreover, the incidence of BC in the world is continuously increasing each year, and it increases with age.[2,3] BC is usually in the mid and late stage when it is diagnosed definitely because of the insidious and atypical symptoms at the early stage of BC.[4] The early diagnosis and treatment of BC are effective measures that can increase survival rates and reduce mortality.[1,5] At present, the main methods to screen and early diagnose BC include imaging examinations, breast biopsy and detection of serum tumor markers.[6] Imaging examinations such as X-ray, computed tomography (CT), magnetic resonance imaging (MRI), positron-emission tomography (PET) and ultrasound have limited value in the early diagnosis of BC, and also rely on expensive testing equipment.[7] Breast biopsy is widely acknowledged as the gold standard for the early diagnosis of BC. But, breast biopsy is an invasive test, which will cause varying degrees of pain for subjects and not suitable for mass screening. Presently, besides imaging examinations and breast biopsy, the detection of

Received: 26 September 2022
Accepted: 3 December 2022
Published: 13 December 2022

serum tumor markers has become a new kind of important method used in early diagnosis of BC, and also is help to improve the detection rate and diagnosis accuracy.[8]

Carbohydrate antigens 15–3 (CA15-3) and carcinoma embryonic antigens (CEA) have been regarded as the most two valuable tumor markers for the early diagnosis and curative effect observation of BC based on their high expression were closely correlated with BC occurrence.[9] It has been shown that the detection of single tumor marker was inadequate for cancer diagnosis due to limited sensitivity and specificity, and the combined detection of CA15-3 and CEA could provide more information for clinical decision-making.[10] Currently, the detection means for CA15-3 and CEA consist mainly of enzyme-linked immunosorbent assay (ELISA), electrochemical immunoassay (ECIA), electrochemiluminescence immunoassay (ECLIA) and so on.[11] However, these detection means have some disadvantages, for instance label needed, consuming long time, low sensitivity and complex operation. Therefore, it is of great significance to develop a reliable multiplex detection method for CA15-3 and CEA with high sensitivity and selectivity, so as to greatly improve the early diagnosis rate and accuracy of BC.

In 2001, the silicon nanowire field-effect transistor (SiNW-FET) was first reported for the detection of biological and chemical molecules.[12] Along with the deepening of research on SiNW-FET biosensors and the development of device fabrication process, the SiNW-FET biosensors have been successfully applied to the detection of various target molecules, such as proteins, nucleic acids, saccharides, viruses, ions and so on.[13] The SiNW-FET biosensors not only effectively overcome the disadvantages of traditional detection methods, but also have been successfully applied in detecting tumor markers with label-free, immediate response, high sensitivity and specificity.[14]

SiNW-FET is a voltage-controlled semiconductor device, the gate voltage is applied to regulate the distribution of majority carriers in the SiNW via the electrical effect, thereby further modulating the conductance of SiNW.[15] Based on the above theory, SiNW-FET can be processed into biosensor for biomolecule detection with high sensitivity and specificity by the surface modification of SiNW with probe molecules which can specifically recognize biomolecules. The detection principle of SiNW-FET biosensor is shown in Figure 1A. The specific binding of electrically charged biomolecules and probe molecules will cause the change of SiNW conductivity, and the change in current between source and drain electrodes will be recorded by a semiconductor analyzer. According to the difference of majority carriers in SiNW, SiNW can be divided into p-type and n-type.[16] For p-type SiNW-FET in which the majority carriers are positively charged electron holes, the specific binding of negatively charged biomolecules and probe molecules will increase the density of electron holes, thereby increasing the conductance and current. The binding of positively charged biomolecules causes the depletion of electron holes to decrease the conductance and current.[17] Conversely, for n-type SiNW-FET in which the majority carriers are negatively charged electrons, the binding of negatively charged biomolecules will decrease the conductance and current, and the binding of positively charged biomolecules will increase the conductance and current.[16]

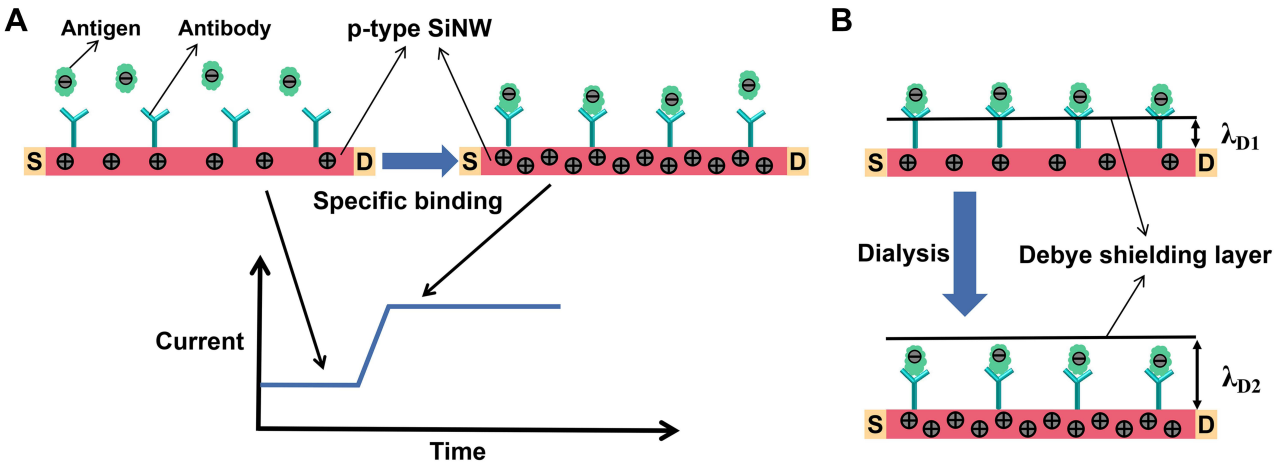

Figure 1 (**A**) The detection principle of SiNW-FET biosensor. (**B**) The principle of overcoming the Debye shielding effect by dialysis.

The SiNW-FET can realize high sensitivity detection for tumor markers in low ionic strength solutions.[18,19] But in high ionic strength physiological solutions (such as untreated serum), the existence of a strong Debye shielding effect will greatly lower the detection sensitivity of SiNW-FET, or even fail it.[20] The intensity of the Debye shielding effect is associated negatively with the Debye length (λ_D), which is defined as $\lambda_D=1/q\times(\varepsilon k_B T/c)^{1/2}$. Where ε, k_B, T, c and q are the permittivity of the media, Boltzmann's constant, the temperature, the ionic strength of the solution and the electron charge, respectively.[21] According to this formula, the λD decreases with the increase of the ionic strength (c). When λ_D is less than the distance from the captured biomolecules to the SiNW surface, the captured biomolecules cannot cause the change of SiNW conductivity and current due to strong Debye shielding effect.[22] In our previous study, we reported a solution for overcoming the Debye shielding effect through the use of a miniature hemodialyzer with volume regulator to desalinate serum, which could effectively decrease the ionic strength of serum and increase the Debye length, thus realizing the detection of tumor markers in serum.[23] The principle of overcoming the Debye shielding effect by dialysis is shown in Figure 1B.

Currently, there are two main fabrication techniques in the preparation of SiNW-FET chips, including "bottom-up" and "top-down" approaches.[24] Due to its inherent limitations, the "bottom-up" approach has low consistency in chip quality and is not conducive to mass production. In contrast, the "top-down" approach has several advantages in mass production, high consistency and low cost.[25] In this study, the multi-channel double-gate SiNW-FET chips for dual-channel detection of BC tumor markers were fabricated by using the top-down semiconductor manufacturing technology. By modifying monoclonal CA15-3 and CEA antibodies separately on the different SiNW surfaces, the SiNW-FET can be used in the dual-channel detection of BC tumor markers CA15-3 and CEA. The multiplexed, highly sensitive and specific detection of CA15-3 and CEA in the phosphate buffer saline (PBS) was successfully realized by the SiNW-FET biosensor. Furthermore, the connection with the miniature hemodialyzer enables the SiNW-FET biosensor to detect CA15-3 and CEA in serum with high sensitivity and specificity. The results of this study indicated that the fabricated SiNW-FET biosensor has the characteristics of mass production, low cost, real-time, repeatability, high sensitivity and specificity. Therefore, the SiNW-FET biosensor used in this work has high clinical application value for the early diagnosis and curative effect observation of BC.

Materials and Methods

Materials

Six-inch p-type (100) silicon-on-insulator (SOI) wafers (ρ:10–20 Ωcm; top silicon layer: 195 nm thick; SiO2 insulating layer: 120 nm thick; silicon substrate: 600 μm thick) were purchased from Shanghai Simgui Co. (Shanghai, China). Polydimethylsiloxan (PDMS) was provided by Dow Corning Co. (Midland, Michigan, USA). 3-Aminopropyltriethoxysilane (APTES), glutaraldehyde (Glu), phosphate buffered saline (PBS; pH 7.4), bovine serum albumin (BSA) and BSA monoclonal antibody were acquired from Sigma-Aldrich (St Louis, MO, USA). CA15-3, CA12-5 and CA15-3 monoclonal antibody were obtained from Alpha Diagnostic Intl. Inc. (San Antonio, Texas, USA). CEA, alpha-fetoprotein (AFP) and their monoclonal antibodies, green fluorescent protein (GFP) and red fluorescent protein (RFP) were purchased from Abcam Inc (Cambridge, MA, USA). The serum samples were collected from female breast cancer patients and healthy female volunteers and stored at 4°C for the short term. The study was approved by the Ethics Committee of the Soochow University and was conducted in accordance with the Declaration of Helsinki. Informed consent was obtained from the patients prior to enrolment in the study.

Fabrication of the Multi-Channel Double-Gate SiNW-FET Chips

The fabrication process for the multi-channel double-gate SiNW-FET chips is shown in Figure 2A. Firstly, the top silicon layer of a six-inch p-type (100) SOI wafer was thinned to 30 nm by thermal oxidation and etching with buffered oxide etch (BOE). Secondly, the nanowires (500 nm wide) and other graphic regions were formed by the UV stepper lithography, and then the top silicon layer and SiO2 insulating layer outside the graphic regions were etched by the reactive ion etching (RIE). The main purpose of this step was to fabricate raised SiNWs (about 500 nm wide and 30 nm high). Thirdly, a specific area of the pattern (including part of SiNW surface) was plated with a 50 nm thick SiO2

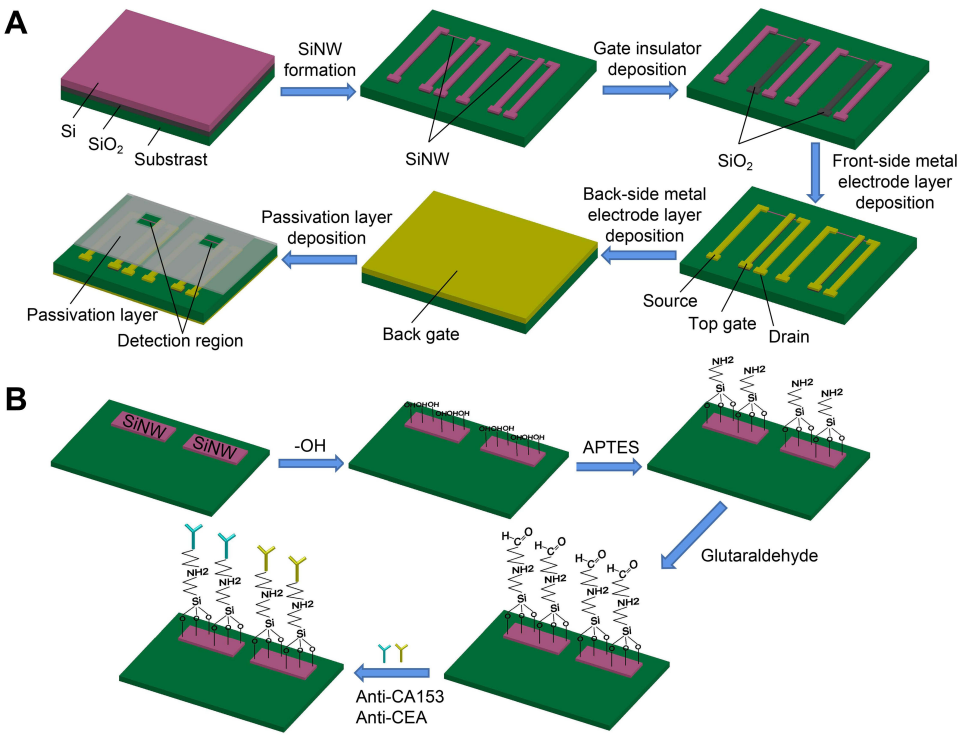

Figure 2 (**A**) The fabrication process for the multi-channel double-gate SiNW-FET chips. (**B**) The functional modification process of the SiNW surfaces.

insulating layer by the method of UV lithography and inductively coupled plasma chemical vapour deposition (ICPCVD). The goal of this step was construct an insulating layer between the top gate electrode and SiNW. Fourthly, a metal electrode layer, which was composed of 5 nm Ti and 100 nm Au, was deposited on the graphic region outside SiNW by the method of UV lithography and physical vapor deposition (PVD) to form the source electrode, drain electrode and top-gate electrode. Fifthly, the back of wafer was coated with a Ti/Au/Ti (5 nm/100 nm/5 nm) metal electrode layer by the PVD method to form the back-gate electrode. Then, the wafer was thermally annealed at 300°C (10°C/S) in quick anneal oven to obtain good ohmic contacts between metal electrode and silicon. Finally, to avoid surface modification of non-detection region and signal interference during detection, the wafer surface other than the reserved detection region was plated with a SiO2/SiNx (100 nm/160 nm) passivation layer by the method of UV lithography and ICPCVD.

Modification of the SiNW-FET with CA15-3 and CEA Antibodies

In this research, CA15-3 and CEA antibodies were separately covalently connected to the different SiNW surfaces on a SiNW-FET chip using the traditional APTES-Glu chemical chain modification method. The functional modification process of the SiNW surfaces is shown in Figure 2B. Firstly, the SiNW-FET chip was successively cleaned with acetone, isopropyl alcohol and deionized water in an ultrasonic cleaner for 10 min, and then dried with nitrogen and cleaned with an oxygen plasma cleaner for 5 min to form a layer of hydroxyl groups on the chip surface. Secondly, the chip was dipped in 2% (v/v) APTES ethanol solution for 45 min to introduce amine groups on the SiNW surfaces. In this process, the oxyethyl groups provided by APTES were combined with hydroxyl groups on the chip surface. Then, the chip was heated at 120°C for an hour to remove unbound APTES molecules. Thirdly, the chip was immersed in 2.5% (v/v) Glutaraldehyde solution for an hour to introduce aldehyde groups on SiNW surfaces in preparation for linking to the amine groups in monoclonal antibody. In this step, the aldehyde groups provided by Glutaraldehyde were combined with the amino groups provided by APTES. Finally, CA153 and CEA antibody (both 100 μg/mL) in PBS solution (pH 7.4) were delivered separately to different SiNW surfaces through the microfluidic channels and kept at 4°C for 4 hours.

PDMS Microfluidic Channels Fabrication and Integration

In this study, we used PDMS to fabricate the microfluidic device, which contains two channels with 7.0 mm in length, 0.6 mm in width and 0.15 mm in height (Figure 3A). Firstly, the dual-channel molds were made on a silicon wafer by the method of UV lithography and silicon deep etching (Figure 3B). Secondly, the PDMS prepolymer and curing agent were fully mixed by weight in the ratio of 10:1, and then the mixture was poured onto the dual-channel molds and placed in a vacuum tank to remove bubbles. Thirdly, the bubble-free mixture was placed at 75°C for 40 min to achieve gradual solidification. Finally, the congealed dual-channel PDMS was separated from the dual-channel silicon molds and drilled by hole punch to obtain the channel of liquid inflow and outflow.

Before integration with the functionalized SiNW-FET, the dual-channel PDMS was successively cleaned with acetone, isopropyl alcohol and deionized water for 10 min, and then dried with nitrogen and cleaned with oxygen plasma for 5 min. Next, the processed dual-channel PDMS was integrated with the functionalized SiNW-FET through reversible encapsulation (Figure 3C), and an acrylic splint was used to fix the integrated SiNW-FET to increase the sealing performance (Figure 3D).

Integration of the Dialyzer with the SiNW-FET Biosensor

A miniature hemodialyzer with volume regulator was made using the dialysis membrane with a total area of 0.01 m^2 and an aperture of 10 K Dalton in this work (Figure 3E). The volume regulator could keep the volume of serum constant before and after dialysis. Before the detection of tumor markers in serum, the miniature hemodialyzer was connected with the SiNW-FET to form Dialysis-SiNW-FET biosensor (Figure 3F). The serum was first desalted and purified by the miniature dialyzer and then flowed through the surface of antibody-modified SiNW-FET.

Measurements of the SiNW-FET Biosensor

All measurements were carried out with an Agilent B1500A Semiconductor Device Analyzer provided by Agilent Technologies Inc. (Santa Clara, CA, USA). A peristaltic pump was used to transport solution to the SiNW-FET biosensor

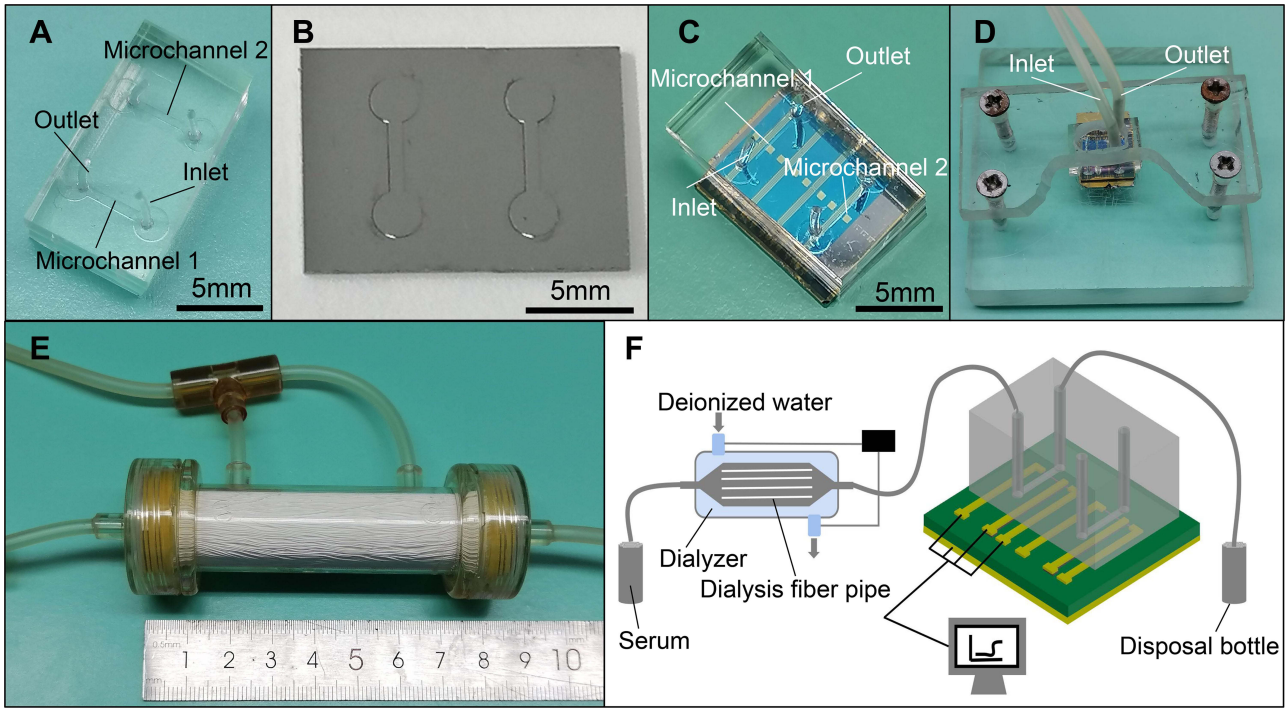

Figure 3 The fabrication of PDMS dual-channel microfluidic device, and the integration of detection system. (**A**) Optical image of the fabricated PDMS dual-channel microfluidic device. (**B**) Optical image of the mold for PDMS microfluidic channels. (**C**) Optical image of the PDMS microfluidic device integrated with the SiNW-FET chip. (**D**) Optical image of the SiNW-FET biosensor integrated with acrylic fastening fixture. (**E**) Optical image of the miniature hemodialyzer with volume regulator. (**F**) Schematic diagram of the detection system.

at a speed of 80 μL/min. All measurements were proceeded at room temperature (25°C±2°C) and repeated for three times.

Results

Structure and Electrical Properties of the Fabricated SiNW-FET

A six-inch SOI wafer can be made into 170 individual SiNW-FET chips. The optical image and structure diagram of a single SiNW-FET chip are shown in Figure 4A and B. The relative positions among SiNW, detection region, source, drain and top-gate can be clearly shown in the optical microscopy image of the SiNW-FET chip (Figure 4C). The scanning electron microscopy (SEM) image show that the width and height of SiNW are approximately 500 nm and 30 nm, respectively (Figure 4D).

The transfer and output characteristics of the fabricated SiNW-FET chips were examined using an Agilent B1500A Semiconductor Device Analyzer. Figure 5A shows the typical transfer characteristic curve of the fabricated chip. When the drain-source voltage (V_{DS}=2V) and back-gate voltage (V_{BG}=1V) were constant, the drain-source current (I_{DS}) increased with the top-gate voltage (V_{TG}) changed from 0V to 10V. The transfer curve illustrates that the fabricated chip has strong gate voltage dependence. Figure 5B shows the output characteristic curve of the fabricated chip. When the back-gate voltage (V_{BG}=1V) was constant, the I_{DS} increased with the V_{DS} changed from 0V to 10V at the different V_{DS}. The above results indicated that the fabricated SiNW-FET chips have excellent electrical performance. The specific binding of negatively charged biomolecules and probe molecules will increase the density of electron holes in SiNW, thereby increasing the I_{DS}.

Surface Functionalization of the Fabricated SiNW-FET

In order to verify the effectiveness of the traditional APTES-Glu chemical chain modification in this study, we used green and red fluorescent proteins (GFP and RFP) instead of CEA and CA15-3 to modify different SiNWs, and then observed the modification results under a fluorescence microscope. Figure 5C and D indicates that GFP and RFP were successfully connected to the different SiNWs. In addition, it is worth pointing out that the SiNW which modified with GFP only show green fluorescence but not red fluorescence, and vice versa. Therefore, it was feasible to connect two different antibodies to the different SiNWs using the current method without affecting the specificity of detection.

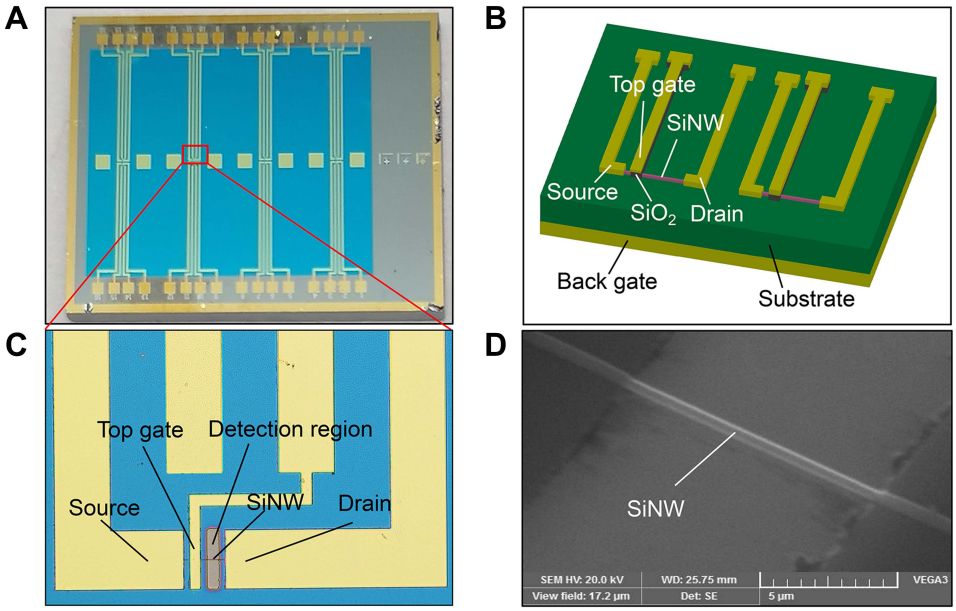

Figure 4 The structure of the multi-channel double-gate SiNW-FET chip. (**A**) Optical image of a single SiNW-FET chip. (**B**) The structure diagram of dual-channel detection on SiNW-FET chip. (**C**) Optical microscope image of the distribution of detection region and electrodes in a single detection channel. (**D**) Scanning electron microscopy image of the fabricated SiNW. The width and height of SiNW is approximately 500 nm and 30 nm, respectively.

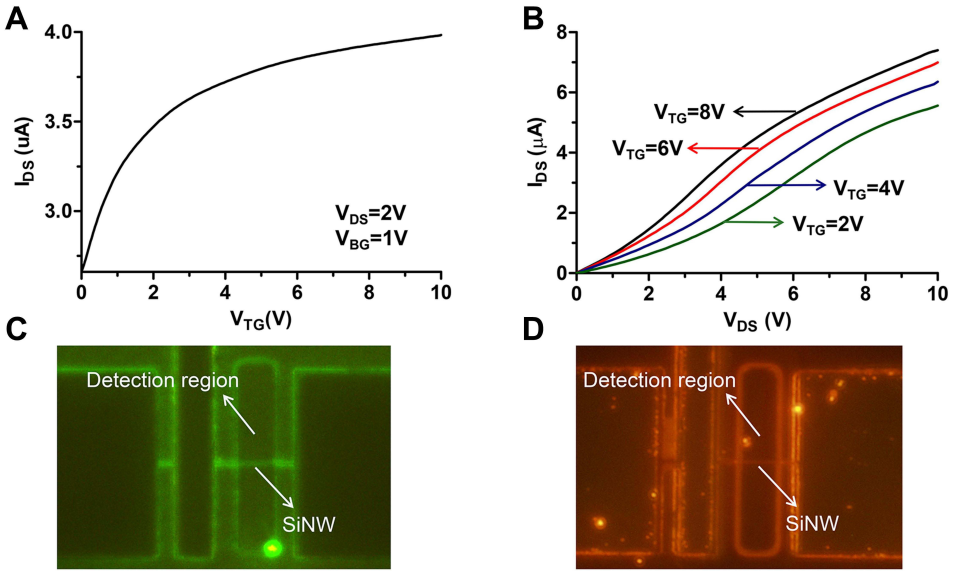

Figure 5 The electrical properties of the SiNW-FET chip, and the results of surface functionalization of SiNW. (**A** and **B**) The transfer and output characteristic curve of the SiNW-FET chip. (**C** and **D**) The results of surface functionalization of different SiNWs using green and red fluorescent proteins.

Specificity and Sensitivity of the Fabricated SiNW-FET Biosensor

The specificity and sensitivity of the fabricated SiNW-FET biosensor were evaluated with CA15-3 and CEA standard solutions, which were obtained by diluting the pure antigens with 0.01×PBS solution. Since the isoelectric point of CA15-3 and CEA are lower than the physiological pH (pH = 7.4), they are negatively charged in serum or PBS solution, and their binding to the specific antibodies will increase the conductance and current of p-type SiNW. When 1U/mL CA15-3 and 1ng/mL CEA were successively pumped into a SiNW-FET biosensor without modified antibodies, no significant current change was observed (as shown in Figure 6A), indicating that there was no non-specific binding of antigen molecules to the SiNW surface. When 1ng/mL CEA and 1U/mL CA12-5 were successively pumped into a SiNW-FET biosensor modified with CA15-3 antibody, there was no significant change of the current, while when 1U/mL CA15-3 was injected into the biosensor, an apparent current change was observed (Figure 6B). Similarly, when 1U/mL CA15-3 and 1ng/mL AFP were successively pumped into a SiNW-FET biosensor modified with CEA antibody, no significant current change was observed. Then, a significant increase in current was observed when 1ng/mL CEA was injected into the biosensor (Figure 6C). The above results indicated that the SiNW-FET biosensor modified with antibody has excellent specificity in the detection of tumor marker.

In order to further detect the sensitivity of the fabricated SiNW-FET biosensor and the relationship between the current change with the concentration of CA15-3 and CEA, a range of known concentrations of CA15-3 and CEA were pumped into the corresponding antibody-modified SiNW-FET. The typical detection results of dual-channel detection of CA15-3 and CEA at different concentrations are shown in Figure 6D and E. The fabricated biosensor exhibited good detection performance with linear ranges of 0.1–10U/mL for CA15-3, 0.01–10 ng/mL for CEA, a detection limit of 0.1U/mL for CA15-3, 0.01 ng/mL for CEA. The results show that the biosensors have high sensitivity for the dual-channel detection of CA15-3 and CEA, which meet the requirement of clinical testing.

Dual-Channel Detection of Breast Cancer Biomarkers CA15-3 and CEA in Serum

The excellent detection ability of the fabricated SiNW-FET biosensor was further examined by detection of CA15-3 and CEA in serum of normal people and breast cancer patients. Figure 6F and G showed the typical detection results of CA15-3 and CEA in the serum of normal person and breast cancer patient, in which the normal serum with a CA15-3 concentration of 10.9 U/mL and a CEA concentration of 2.67 ng/mL, the serum of breast cancer patient with a CA15-3 concentration of 45.8 U/mL and a CEA concentration of 10.24 ng/mL. The concentration of CA15-3 and CEA in serum were measured using a Roche Elecsys 2010 electrochemiluminescence immunoassay analyzer provided by Roche

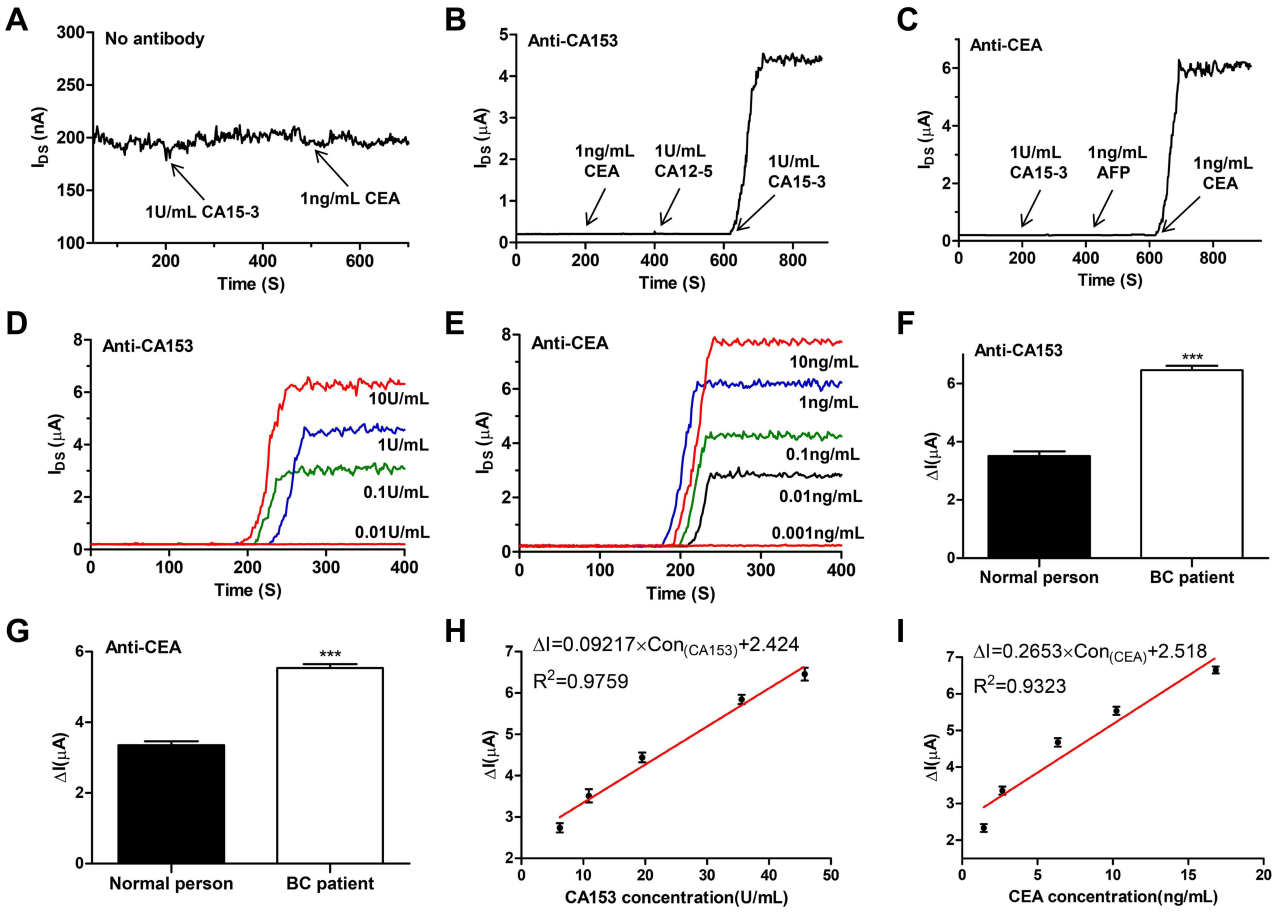

Figure 6 The specificity and sensitivity of the SiNW-FET biosensor, and the results of dual-channel detection of CA15-3 and CEA in the dialyzed serum samples. (**A**) Plot of current versus time when 0.5mg/mL BSA, 1U/mL CA15-3 and 1ng/mL CEA in 0.01×PBS solution were successively pumped into unmodified SiNW-FET biosensor. (**B** and **C**) Plot of current versus time for the anti-CA15-3 and anti-CEA SiNW-FET biosensor. (**D**) The anti-CA15-3 SiNW-FET biosensor response to different concentrations of CA15-3 in 0.01×PBS solution. (**E**) The anti-CEA SiNW-FET biosensor response to different concentrations of CEA in 0.01×PBS solution. (**F** and **G**) Response of the anti-CA15-3 and anti-CEA SiNW-FET biosensor to the dialyzed serum samples. ***$p < 0.001$. (**H** and **I**) The current change (ΔI) versus the CA15-3 and CEA concentrations in the dialyzed serum samples.

Diagnostics GmbH. The detection results show that breast cancer patient serum resulted in much more obvious current change than normal people serum. Figure 6H and I showed the relationship between current change (ΔI) and the concentration of CA15-3 and CEA in serum.

Discussion

In this work, the dual-gate SiNW-FET chips were fabricated using the top-down semiconductor manufacturing technology, which has advantages in mass production, high consistency and low cost.[25] A six-inch SOI wafer can be made into about 170 individual chips. In addition, the dual-gate SiNW-FET can amplify the detection signal by multiples through the capacitive-coupling effect, thereby increase the signal-to-noise ratio of SiNW-FET.[26] The detection results of standard solutions show that the prepared biosensors have high specificity and sensitivity. In order to achieve the dual-channel detection of CA15-3 and CEA, the traditional APTES-Glu chemical chain modification method was used to modify monoclonal antibodies onto the different SiNW surfaces,[27] and the dual-channel PDMS microfluidic device was used to transport solution containing monoclonal antibodies or tumor markers to the function area. The application of dual-channel PDMS microfluidic device not only improved the accuracy of antibody modification, but also effectively avoided the mutual interference between the two groups and increased the reliability of detection.

In order to further improve the specificity and sensitivity of the prepared biosensor, we used the BSA blocking method to occlude the non-specific protein adsorption sites on the surface of PDMS microchannels and minimize non-

specific adsorption interference.[28,29] About 300 uL 0.01×PBS solution containing 0.5mg/mL BSA was first pumped through detection region to obtain a stable baseline current (I_0) and block the non-specific protein adsorption sites on the surface of PDMS microchannels. Moreover, previous study has suggested that the detection sensitivity of SiNW-FET can reach optimal level in the subthreshold regime.[30] Therefore, we applied V_{DS} = 2 V, V_{TG} = 2 V, V_{BG} = 1 V for detection, letting the fabricated SiNW-FET working in the subthreshold regime. To decrease the adverse effect on the detection caused by the Debye shielding effect, the detection for CA15-3 and CEA standard solutions was carried out in 0.01×PBS solution.

Previous research has suggested that the existence of a strong Debye shielding effect in serum would greatly lower the detection sensitivity of SiNW-FET.[31] Several methods have been proposed to reduce the influence of Debye shielding effect on the detection of tumor markers in serum, mainly including dilution,[32] protein purification,[33] tailoring antibody and aptamer substitution method.[21,34] The serum dialysis method was used in this study to overcome the Debye shielding effect. The serum was first desalted and purified by the miniature dialyzer and then pumped into the antibody-modified SiNW-FET. The miniature dialyzer with volume regulator could decrease ionic strength while keeping the concentration of tumor markers and serum volume constant. The results showed that the prepared SiNW-FET biosensor could not only detect tumor markers in serum with high sensitivity, but also distinguish the difference in serum concentration of tumor markers between normal people and breast cancer patients.

CA15-3 and CEA are the most two valuable tumor markers for the early diagnosis and curative effect observation of BC, and their concentrations in normal people serum are generally less than 30U/mL and 5ng/mL, respectively.[35,36] Currently, there are many types of sensors for detecting CA15-3 and CEA, and each one has its own superiorities. In order to more intuitively compare the detection performance of CA15-3 and CEA sensors based on different methods, the relevant data from published literatures and the results of this study are summarized in Table 1 [37–40] and Table 2.[38,41–44] Although the linear range and low detection limit for CA153 and CEA detection were not as good as fluorescence

Table 1 Comparison of the Performance of Various Sensors for CA15-3 Detection

Methods	Materials	Detection Limit (U/mL)	Linear Range (U/mL)	Response Time	References
FIA	MoS2 nanosheets	0.0039	0.01–0.1	10min	[37]
ECIA	AuCs/GR	0.0015	0.005–50	25min	[38]
ECLIA	ZNs-PAMAM	0.033	0.1–120	30min	[39]
GDY-FET	Graphdiyne	0.043×10^{-9}	1×10^{-9}-1×10^{-5}	Instant response	[40]
DG SiNW-FET	SiNW	0.1	0.1–10	Instant response	This work

Abbreviations: FIA, fluorescence immunoassay; ECIA, electrochemical immunoassay; AuCs/GR, gold clusters/graphene; ECLIA, electrochemiluminescence immunoassay; ZNs-PAMAM, polyamidoamine-functionalized ZnO nanorods; GDY-FET, graphdiyne silicon nanowire field effect transistor; DG SiNW-FET, double-gate silicon nanowire field effect transistor.

Table 2 Comparison of the Performance of Various Sensors for CEA Detection

Methods	Materials	Detection Limit (ng/mL)	Linear Range (ng/mL)	Response Time	References
FIA	UCNPs/GO	0.0079	0.03–6	10min	[41]
ECIA	AuCs/GR	0.0012	0.004–200	25min	[38]
ECLIA	PANI/PPy-Ag	0.0004	0.001–100	50min	[42]
G-FET	Graphene	0.1	0.1–100	Instant response	[43]
Si-NR FET	SiNR	0.01	0.01–10	Instant response	[44]
DG SiNW-FET	SiNW	0.01	0.01–10	Instant response	This work

Abbreviations: FIA, fluorescence immunoassay; UCNPs/GO, upconversion nanoparticles/graphene oxide; ECIA, electrochemical immunoassay; AuCs/GR, gold clusters/graphene; ECLIA, electrochemiluminescence immunoassay; PANI/PPy-Ag, Polyaniline/polypyrrole-silver; G-FET, graphene field effect transistor; Si-NR FET, silicon nanoribbon field effect transistor field effect transistor; DG SiNW-FET, double-gate silicon nanowire field effect transistor.

immunoassay (FIA), ECIA and ECLIA, the above three methods need a long response time, while the prepared SiNW-FET can respond instantly. Compared to CEA detection, the prepared SiNW-FET biosensor possesses similar detection performance with other types FET biosensor. Importantly, the prepared SiNW-FET biosensor has high sensitivity, specificity and repeatability for the dual-channel detection of CA15-3 and CEA, which can meet the requirements of clinical application.

Conclusions

In conclusion, the present study reported a SiNW-FET biosensor for high sensitive and high selective dual-channel detection of breast cancer biomarkers CA15-3 and CEA in serum. The fabricated SiNW-FET biosensors were demonstrated for detecting as low as 0.1U/mL CA15-3 and 0.01 ng/mL CEA. Moreover, the biosensors were able to distinguish the difference of tumor markers concentration in serum between normal people and breast cancer patients, which further demonstrating its excellent detection performance. The results of this study demonstrate that the fabricated multi-channel SiNW-FET biosensors have potential to be an effective tool in the early diagnosis and curative effect observation of BC.

Acknowledgments

This work was supported by grants from the Health Science and Technology Innovation Project of Suzhou Science and Technology Bureau (No. SKYD2022068) and the Scientific Research Foundation of Suzhou Ninth Hospital Affiliated to Soochow University (No. YK202201).

Disclosure

The authors report no conflicts of interest in this work.

References

1. Trapani D, Ginsburg O, Fadelu T, et al. Global challenges and policy solutions in breast cancer control. *Cancer Treat Rev*. 2022;104:102339. doi:10.1016/j.ctrv.2022.102339
2. Houghton SC, Hankinson SE. Cancer progress and priorities: breast cancer. *Cancer Epidemiol Biomarkers Prev*. 2021;30:822–844. doi:10.1158/1055-9965.EPI-20-1193
3. Chan WL, Marinho J, Chavarri-Guerra Y, et al. Systemic treatment for triple negative breast cancer in older patients: a Young International Society of Geriatric Oncology Review Paper. *J Geriatr Oncol*. 2022;13:563–571. doi:10.1016/j.jgo.2022.01.002
4. Albeshan SM, Hossain SZ, Mackey MG, et al. Can breast self-examination and clinical breast examination along with increasing breast awareness facilitate earlier detection of breast cancer in populations with advanced stages at diagnosis? *Clin Breast Cancer*. 2020;20:194–200. doi:10.1016/j.clbc.2020.02.001
5. He Z, Chen Z, Tan M, et al. A review on methods for diagnosis of breast cancer cells and tissues. *Cell Prolif*. 2020;53:e12822. doi:10.1111/cpr.12822
6. Pesapane F, Suter MB, Rotili A, et al. Will traditional biopsy be substituted by radiomics and liquid biopsy for breast cancer diagnosis and characterisation? *Med Oncol*. 2020;37:29. doi:10.1007/s12032-020-01353-1
7. Jafari SH, Saadatpour Z, Salmaninejad A, et al. Breast cancer diagnosis: imaging techniques and biochemical markers. *J Cell Physiol*. 2018;233:5200–5213. doi:10.1002/jcp.26379
8. Bayo J, Castano MA, Rivera F, et al. Analysis of blood markers for early breast cancer diagnosis. *Clin Transl Oncol*. 2018;20:467–475. doi:10.1007/s12094-017-1731-1
9. Song X, Liang B, Wang C, et al. Clinical value of color Doppler ultrasound combined with serum CA153, CEA and TSGF detection in the diagnosis of breast cancer. *Exp Ther Med*. 2020;20:1822–1828. doi:10.3892/etm.2020.8868
10. Fu Y, Li H. Assessing clinical significance of serum CA15-3 and Carcinoembryonic Antigen (CEA) levels in breast cancer patients: a meta-analysis. *Med Sci Monit*. 2016;22:3154–3162. doi:10.12659/MSM.896563
11. Laraib U, Sargazi S, Rahdar A, et al. Nanotechnology-based approaches for effective detection of tumor markers: a comprehensive state-of-The-art review. *Int J Biol Macromol*. 2022;195:356–383. doi:10.1016/j.ijbiomac.2021.12.052
12. Cui Y, Wei Q, Park H, et al. Nanowire nanosensors for highly sensitive and selective detection of biological and chemical species. *Science*. 2001;293:1289–1292. doi:10.1126/science.1062711
13. Noor MO, Krull UJ. Silicon nanowires as field-effect transducers for biosensor development: a review. *Anal Chim Acta*. 2014;825:1–25. doi:10.1016/j.aca.2014.03.016
14. Lee M, Palanisamy S, Zhou BH, et al. Ultrasensitive electrical detection of follicle-stimulating hormone using a functionalized silicon nanowire transistor chemosensor. *ACS Appl Mater Interfaces*. 2018;10:36120–36127. doi:10.1021/acsami.8b11882
15. Pachauri V, Ingebrandt S. Biologically sensitive field-effect transistors: from ISFETs to NanoFETs. *Essays Biochem*. 2016;60:81–90. doi:10.1042/EBC20150009
16. Zhang GJ, Ning Y. Silicon nanowire biosensor and its applications in disease diagnostics: a review. *Anal Chim Acta*. 2012;749:1–15. doi:10.1016/j.aca.2012.08.035
17. Li BR, Chen CC, Kumar UR, et al. Advances in nanowire transistors for biological analysis and cellular investigation. *Analyst*. 2014;139:1589–1608. doi:10.1039/c3an01861j

18. Zhu K, Zhang Y, Li Z, et al. Simultaneous detection of alpha-fetoprotein and carcinoembryonic antigen based on si nanowire field-effect transistors. *Sensors*. 2015;15:19225–19236. doi:10.3390/s150819225
19. Kim K, Park C, Kwon D, et al. Silicon nanowire biosensors for detection of cardiac troponin I (cTnI) with high sensitivity. *Biosens Bioelectron*. 2016;77:695–701. doi:10.1016/j.bios.2015.10.008
20. Nakatsuka N, Yang KA, Abendroth JM, et al. Aptamer-field-effect transistors overcome Debye length limitations for small-molecule sensing. *Science*. 2018;362:319–324. doi:10.1126/science.aao6750
21. Elnathan R, Kwiat M, Pevzner A, et al. Biorecognition layer engineering: overcoming screening limitations of nanowire-based FET devices. *Nano Lett*. 2012;12:5245–5254. doi:10.1021/nl302434w
22. Kesler V, Murmann B, Soh HT. Going beyond the debye length: overcoming charge screening limitations in next-generation bioelectronic sensors. *Acs Nano*. 2020;14:16194–16201. doi:10.1021/acsnano.0c08622
23. Chen H, Zhao X, Xi Z, et al. A new biosensor detection system to overcome the Debye screening effect: dialysis-silicon nanowire field effect transistor. *Int J Nanomedicine*. 2019;14:2985–2993. doi:10.2147/IJN.S198734
24. Tintelott M, Pachauri V, Ingebrandt S, et al. Process variability in top-down fabrication of silicon nanowire-based biosensor arrays. *Sensors*. 2021;21:5153. doi:10.3390/s21155153
25. Tran DP, Pham T, Wolfrum B, et al. CMOS-compatible silicon nanowire field-effect transistor biosensor: technology development toward commercialization. *Materials*. 2018;11:785. doi:10.3390/ma11050785
26. Lim CM, Lee IK, Lee KJ, et al. Improved sensing characteristics of dual-gate transistor sensor using silicon nanowire arrays defined by nanoimprint lithography. *Sci Technol Adv Mater*. 2017;18:17–25. doi:10.1080/14686996.2016.1253409
27. Chua JH, Chee RE, Agarwal A, et al. Label-free electrical detection of cardiac biomarker with complementary metal-oxide semiconductor-compatible silicon nanowire sensor arrays. *Anal Chem*. 2009;81:6266–6271. doi:10.1021/ac901157x
28. Kong T, Su R, Zhang B, et al. CMOS-compatible, label-free silicon-nanowire biosensors to detect cardiac troponin I for acute myocardial infarction diagnosis. *Biosens Bioelectron*. 2012;34:267–272. doi:10.1016/j.bios.2012.02.019
29. Hideshima S, Sato R, Inoue S, et al. Detection of tumor marker in blood serum using antibody-modified field effect transistor with optimized BSA blocking. *Sensors Actuators B*. 2012;161:146–150. doi:10.1016/j.snb.2011.10.001
30. Gao XP, Zheng G, Lieber CM. Subthreshold regime has the optimal sensitivity for nanowire FET biosensors. *Nano Lett*. 2010;10:547–552. doi:10.1021/nl9034219
31. Krivitsky V, Zverzhinetsky M, Patolsky F. Antigen-dissociation from antibody-modified nanotransistor sensor arrays as a direct biomarker detection method in unprocessed biosamples. *Nano Lett*. 2016;16:6272–6281. doi:10.1021/acs.nanolett.6b02584
32. Gao A, Yang X, Tong J, et al. Multiplexed detection of lung cancer biomarkers in patients serum with CMOS-compatible silicon nanowire arrays. *Biosens Bioelectron*. 2017;91:482–488. doi:10.1016/j.bios.2016.12.072
33. Stern E, Vacic A, Rajan NK, et al. Label-free biomarker detection from whole blood. *Nat Nanotechnol*. 2010;5:138–142. doi:10.1038/nnano.2009.353
34. Lee HS, Kim KS, Kim CJ, et al. Electrical detection of VEGFs for cancer diagnoses using anti-vascular endotherial growth factor aptamer-modified Si nanowire FETs. *Biosens Bioelectron*. 2009;24:1801–1805. doi:10.1016/j.bios.2008.08.036
35. Compton C, Fenoglio-Preiser CM, Pettigrew N, et al. American joint committee on cancer prognostic factors consensus conference: colorectal working group. *Cancer Am Cancer Soc*. 2000;88:1739–1757.
36. Ishibashi N, Maebayashi T, Aizawa T, et al. Serum tumor marker levels at the development of intracranial metastasis in patients with lung or breast cancer. *J Thorac Dis*. 2019;11:1765–1771. doi:10.21037/jtd.2019.05.37
37. Zhao L, Kong D, Wu Z, et al. Interface interaction of MoS2 nanosheets with DNA based aptameric biosensor for carbohydrate antigen 15-3 detection. *Microchem J*. 2020;155:104675. doi:10.1016/j.microc.2020.104675
38. Ge S, Yu F, Ge L, et al. Disposable electrochemical immunosensor for simultaneous assay of a panel of breast cancer tumor markers. *Analyst*. 2012;137(20):4727–4733. doi:10.1039/c2an35967g
39. Jiang X, Wang H, Yuan R, et al. Sensitive electrochemiluminescence detection for CA15-3 based on immobilizing luminol on dendrimer functionalized ZnO nanorods. *Biosens Bioelectron*. 2015;63:33–38. doi:10.1016/j.bios.2014.07.009
40. Ghafary Z, Salimi A, Hallaj R. Exploring the role of 2D-graphdiyne as a charge carrier layer in field-effect transistors for non-covalent biological immobilization against human diseases. *Acs Biomater Sci Eng*. 2022;8:3986–4001. doi:10.1021/acsbiomaterials.2c00607
41. Wang Y, Wei Z, Luo X, et al. An ultrasensitive homogeneous aptasensor for carcinoembryonic antigen based on upconversion fluorescence resonance energy transfer. *Talanta*. 2019;195:33–39. doi:10.1016/j.talanta.2018.11.011
42. Zhang L, Wang Y, Shen L, et al. Electrochemiluminescence behavior of AgNCs and its application in immunosensors based on PANI/PPy-Ag dendrite-modified electrode. *Analyst*. 2017;142:2587–2594. doi:10.1039/C7AN00443E
43. Zhou L, Mao H, Wu C, et al. Label-free graphene biosensor targeting cancer molecules based on non-covalent modification. *Biosens Bioelectron*. 2017;87:701–707. doi:10.1016/j.bios.2016.09.025
44. Bao Z, Sun J, Zhao X, et al. Top-down nanofabrication of silicon nanoribbon field effect transistor (Si-NR FET) for carcinoembryonic antigen detection. *Int J Nanomedicine*. 2017;12:4623–4631. doi:10.2147/IJN.S135985